GEODEZJA I KARTOGRAFIA
GEODESY AND CARTOGRAPHY
Vol. 56, No 1, 2007, pp. 21-35

Mathematical model for bundle block adjustment of HRS images described by Keplerian parameters with orbital constraints

Luong Chinh Ke

Warsaw University of Technology
Institute of Photogrammetry and Cartography
1 Plac Politechniki, 00-661 Warsaw, Poland
e-mail: lchinhke@gazeta.pl

Received: 3 April 2007/Accepted: 28 June 2007

Abstract: Nowadays, an orthomap destined for different purposes can be created from High Resolution Satellite (HRS) images using IKONOS, QuickBird and other satellite imageries having Ground Sampling Distance (GSD) lower than 1 m. The orthomap is one of the main sources for establishing GIS. Accuracy of the orthomap depends first of all on the parameters of Ground Control Points (GCPs) (the forms, number, accuracy and their distribution). In order to reduce the cost and number of GCP field measurements, the block of HRS images has been proposed. The accuracies of determined points in the block of HRS images are affected by the mathematical model used to build a block. The paper presents a general algorithm of bundle block adjustment model of HRS images using Keplerian parameters. In order to overcome strong correlation among exterior orientation elements of HRS images that causes the normal equation ill-conditioned, the ridge-stein estimator and orbital addition constraints have been proposed.

Keywords: High Resolution Satellite image, parametrical or physical model, replacement sensor model, block adjustment, co-linearity condition

1. Introduction

In 4 October 2007 there will be the 50-th anniversary when first time in human history the satellite SPUTNIK-1 of the Soviet Union was launched. The date of 4 October 1957 marked the beginning of new era of human ability to conquer the universe. 20 months later, in 1959, the US tests of the CORONA system started. The state of the art in that time allowed only the use of a film for imaging. The USA used the film up to 1963 and declassified its images in 1995, but Russia made the last satellite photo flight in 2000.

In 1972, the first civil satellite for Earth surface mapping with the use of digital technology – called Earth Resources Technology Satellite (ERTS), later renamed to Landsat-1, constructed by USA, was launched. First digital images acquired from Landsat-1 were already presented on the ISPRS Congress in Ottawa, Canada in 1972. Landsat-1 initiated the era of the new technique in digital form acquiring Earth in-

formation from space. The Multispectral Scanner System (MMS) sensor of Landsat-1 provided a spatial resolution of 80 m and a swath width of 185 km. Landsat-4 (1982) with Thematic Mapper (TM) system give ground sampling distance (GSD) of 30 m. Landsat-7 (1999) with improved TM system has GSD of 15 m. In September 1999 SpaceImaging Company (USA) launched the IKONOS-2 satellite with GSD of 0.82 m. Later, two companies: Earth Watch and OrbImage (USA) put in orbits QuickBird-2 (2002) with GSD of 0.61 m for PAN image, 2.44 m for MS image and OrbView-3 (2002) with GSD of 1 m for PAN image, 4 m for MS image, respectively (Jacobsen, 2005). In 1986-2002 a series of SPOT satellites of France were launched into space. GSD for PAN images of SPOT1, SPOT2, SPOT4 is 10 m. SPOT5 has two sensors with GSD of 5 m and 2.5 m. Some satellite systems of different countries with GSD from 2 m to 39 m (medium resolution satellite images – MRS), in the period 2006–2012, are represented in Figure 1.

Pléaides imageries (France, 2009) with GSD of 0.71 m, WorldView and GeoEye imageries (USA, 2007) of GSD of 0.47 m and 0.41 m, respectively, as well as other commercial systems having GSD below 0.5 m will appear on the world market in the near future. They create a new trend of utilization of super high resolution satellite (SHRS) imageries with GSD $\leq$ 0.5 m for large scale (1:5 000 – 1:2 000) mapping, for generating orthomaps of 0.5 m pixel and DEM of 1.0 m vertical accuracy. Eight countries such as USA, India, Israel, France, South Korea, Italy, Germany and Russia can support the images with GSD $\leq$ 1 m (Fig. 2). Images with GSD up to 2.5 m can be provided by five countries: United Kingdom, Thailand, Brazil, China, and Malaysia.

For last five years the study on geometrical models of HRS imageries has been carried out in different research institutions in the world. Parametrical (or physical) model based on Kepler's laws of satellite motion describes directly strict geometrical relations between the terrain and its image with the use of the co-linearity condition. Such model considers the multi-source distorting factors (Dowman and Michalis, 2003; Michalis and Dowman, 2004, 2005; Luong and Wolniewicz, 2005a, 2005b; Wolniewicz and Luong, 2006).

Replacement model is to provide a simple, generic set of equations to accurately represent the ground-to-image relationship of the physical camera (Dial and Grodecki, 2005). In practice, the Rational Polynomial Coefficients (RPC) model and other models of high resolution satellite that represent the indirect relation between the terrain and its image acquired in the flight orbit have been described (Grodecki et al., 2003; Yamakawa and Fraser, 2004).

In order to generate orthomaps from HRS images the number of ground control points (GCP) is needed for their orthorectifying (Kaczynski and Ewiak, 2005). GCP can be determined in the field by traditional surveying or satellite navigation using e.g. the DGPS technique. In order to reduce the cost and number of GCP field measurements the block of HRS images has been proposed. The accuracies of determined points in the block of HRS images should be satisfactory for orthorectifying and other applications. In the beginning of 21 century different research institutions in the world have concentrated on block adjustment of HRS images using generic sensor model such

as RPC (Dial and Grodecki, 2003, 2004; Grodecki et al., 2003, 2004; James, 2004; Madami, 2005; Passini and Jacobsen, 2006; Passini et al., 2005) or parallel projection model (Zhang et al., 2004).

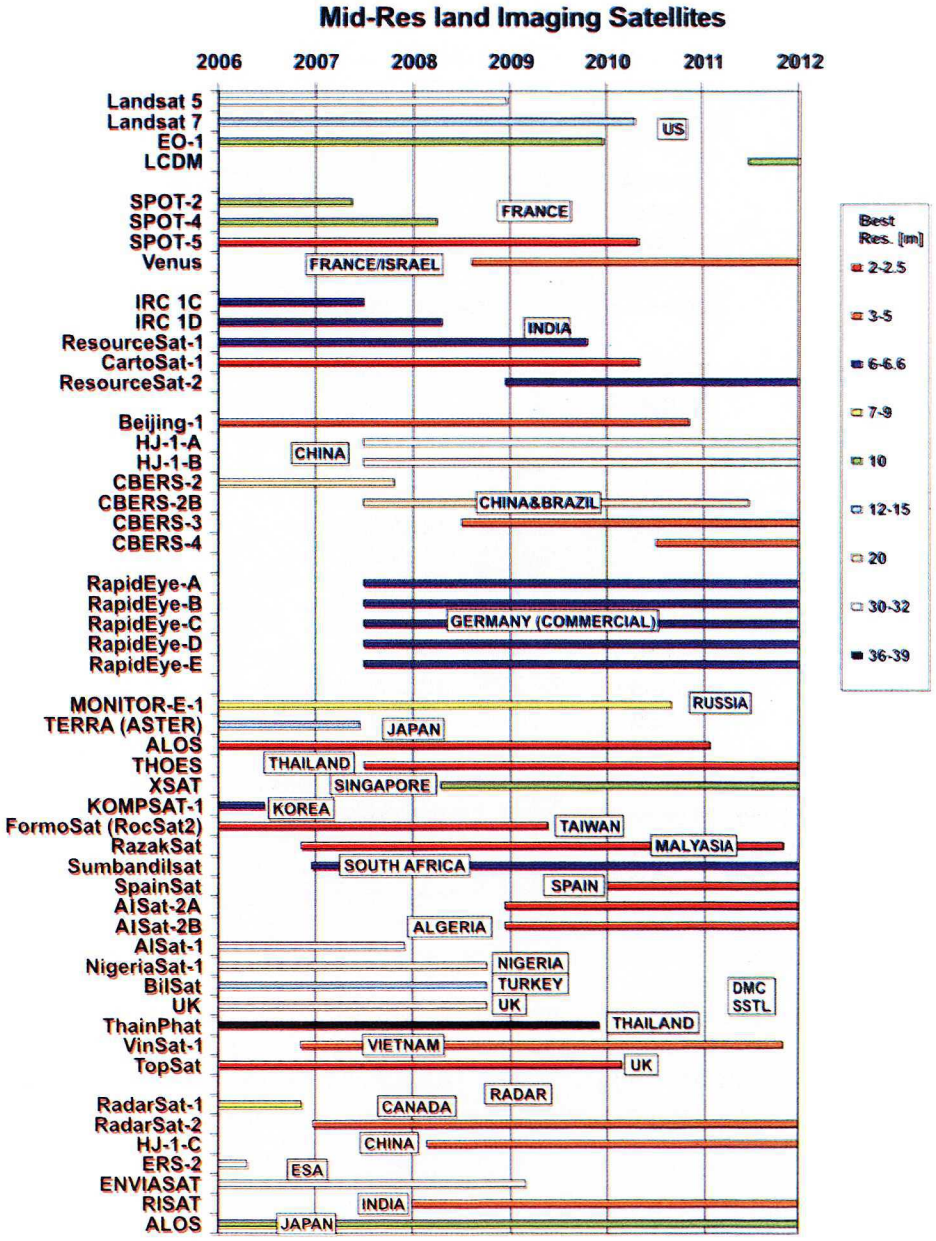

Fig. 1. MRS images available actually and in near future (source: www.asprs.org)

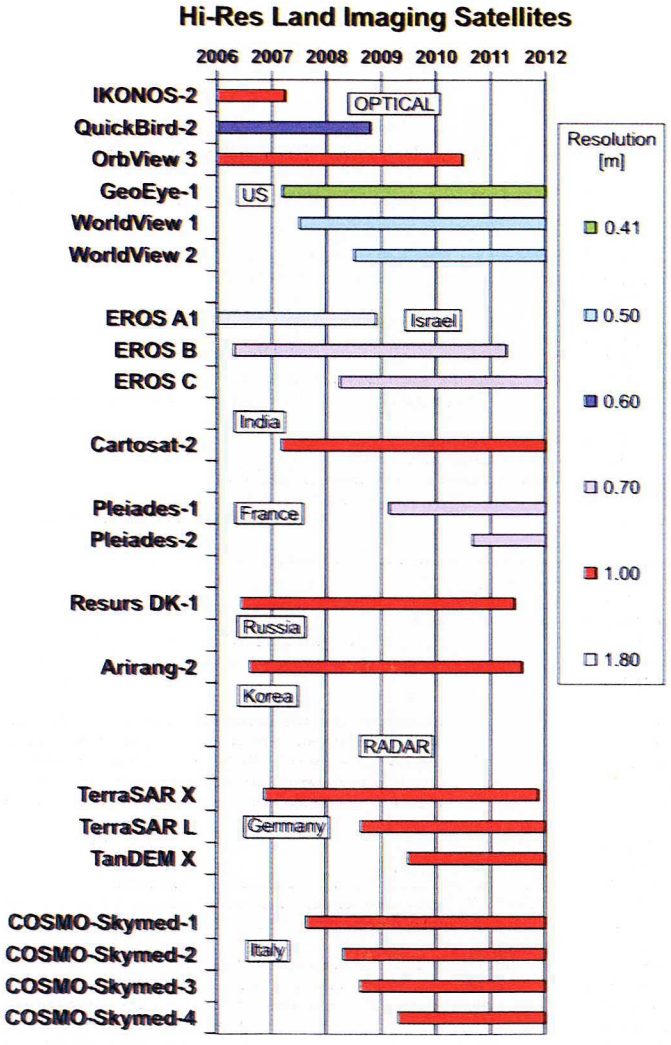

Fig. 2. HRS images available actually and in near future (source: www.asprs.org)

In the Institute of Photogrammetry and Cartography of the Warsaw University of Technology, rigorous block triangulation from HRS images based on Keplerian parameters (parametrical or physical model) has been carried out. In this paper the theoretical algorithm of rigorous block adjustment for HRS images is discussed.

2. Keplerian model of HRS image

Supposed the ground point Q has spatial coordinates X_L, Y_L, Z_L, and X, Y, Z in the local geodetic system $OX_LY_LZ_L$ and in the geocentric system $OXYZ$, respectively. Its corresponding position q on image, taken from elliptic orbit of a satellite S at a time

epoch t has coordinates x, y, $-f$ in the image system $oxyz$ (Fig. 3). Four angular parameters (orbital elements) that determine orbit position in space with respect to Earth's equatorial plane are i – orbit inclination, Ω – longitude of the ascending node, w – the argument of perigee, and ϑ – true anomaly of satellite at epoch t. Next two parameters of satellite orbit are eccentricity e and semi-major axis a that define orbit's shape and size. Satellite position in the given orbit can also be determined by its radius $r = OO' + O'S = R + H$ (R – Earth's radius, H – satellite altitude) and true anomaly ϑ. The coordinates of image point that were corrected with the errors of sensor interiors elements taken from calibration and of along-track view angle θ of sensor optical axis such as IKONOS, QuickBird, or across-track view angle α as SPOT1-SPOT4, IRS will be denoted as x_{ct}, y_{ct}, z_{ct} (Luong and Wolniewicz, 2005a, 2005b, 2006).

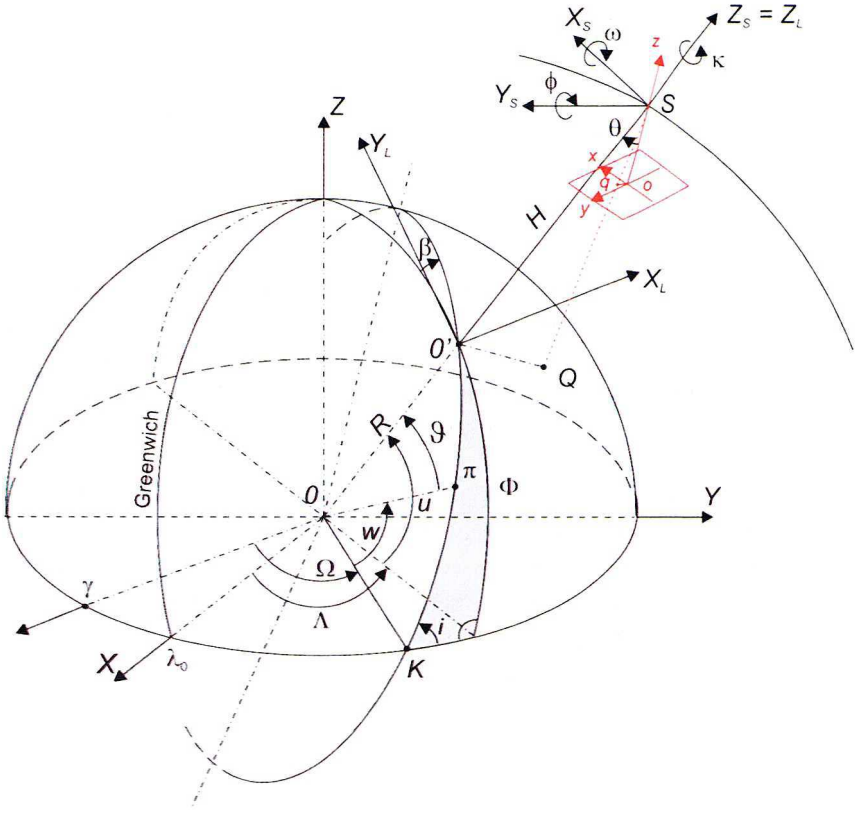

Fig. 3. Geometrical relationship between imagery and its terrain in the geocentric system $OXYZ$

The remaining symbols in Figure 3 mean: γ – vernal equinox, λ_0 – Greenwich meridian, K – ascending node, π – perigee, Λ – geocentric longitude of the satellite, Φ – geocentric latitude of the satellite.

Basing on the co-linearity condition there is the following relation:

$$x_{ct} = z_{ct}\frac{a_1(t)[X - X_S(t)] + a_2(t)[Y - Y_S(t)] + a_3(t)[Z - Z_S(t)]}{a_7(t)[X - X_S(t)] + a_8(t)[Y - Y_S(t)] + a_9(t)[Z - Z_S(t)]}$$
$$y_{ct} = z_{ct}\frac{a_4(t)[X - X_S(t)] + a_5(t)[Y - Y_S(t)] + a_6(t)[Z - Z_S(t)]}{a_7(t)[X - X_S(t)] + a_8(t)[Y - Y_S(t)] + a_9(t)[Z - Z_S(t)]} \quad (1a)$$

where

$$\begin{bmatrix} x_{ct} \\ y_{ct} \\ z_{ct} \end{bmatrix} = R_{\theta(\text{or }\alpha)} \begin{bmatrix} x - (dx_o + \Delta x) \\ y - (dy_o + \Delta y) \\ -(f + df) \end{bmatrix} \quad (1b)$$

$$dx = dx_o + \Delta x = dx_o + \frac{x}{f}df + t_1 x r_a^2 + t_2 x r_a^4 + t_3 x r_a^6 + p_1(y^2 + 3x^2) + p_2 2xy$$

with (1c)

$$dy = dy_o + \Delta y = dy_o + \frac{y}{f}df + t_1 y r_a^2 + t_2 y r_a^4 + t_3 y r_a^6 + p_1 2xy + p_2(x^2 + 3y^2)$$

where dx_o, dy_o, df are sensor's internal orientation errors, t_1, t_2, t_3 are coefficients charactering error of symmetrical distortion, $r_a = oq$ is the radial distance of q from the image centre o, and p_1, p_2 are coefficients charactering error of asymmetrical distortion of optical sensor. Both dx and dy may be considered equal to 0 when they do not exceed the values required in calibration. For simplification, in further considerations $dx = 0$ and $dy = 0$ were used.

In (1a) the coefficients $a_i(t)$ ($i = 1, 2, 3, \ldots, 9$) are the elements of rotational matrix of CCD array line; they are functions of image exterior orientation elements ω, φ, κ and orbital angular parameters Ω, i, u (where $u = w + \vartheta$) at epoch t. Further $X_S(t)$, $Y_S(t)$, $Z_S(t)$ are the coordinates of the perspective centre S at epoch t; they are also functions of satellite orbit parameters. Considering (1a) and (1b), the new general form for dynamic image taken from elliptic orbit with along-track view angle θ at epoch t is:

$$F_{xt}[x,\ f,\ X,\ Y,\ Z,\ \theta,\ \omega(t),\ \varphi(t),\ \kappa(t),\ i(t),\ \Omega(t),\ u(t),\ r(t)] = 0$$
$$F_{yt}[y,\ f,\ X,\ Y,\ Z,\ \theta,\ \omega(t),\ \varphi(t),\ \kappa(t),\ i(t),\ \Omega(t),\ u(t),\ r(t)] = 0 \quad (2)$$

According to (2) each CCD array line has 7 unknown parameters ω, φ, κ, i, Ω, u, r. IKONOS and QuickBird scenes have 3454 and 8656 lines, respectively. There is a large number of unknown parameters to be determined for one scene what practically makes impossible to obtain the solution. In order to solve (2), the unknown parameters are considered as functions of time t or functions of CCD array lines l based on polynomial form of second order. It means

$$U_j(t) = \sum_{i=0}^{2} c_{i,j} t^i \equiv \sum_{i=0}^{2} d_{i,j} l^i \tag{3}$$

where $\mathbf{U}^{\mathrm{T}}(t) = [\omega(t), \varphi(t), \kappa(t), i(t), \Omega(t), u(t), r(t)]$ is the vector of unknown parameters.

Orbital parameters (a, e, i, Ω, w) can be determined using given position vector $(X_o, Y_o, Z_o)^{\mathrm{T}}$ and velocity vector $(v_x, v_y, v_z)^{\mathrm{T}}$ of the satellite (satellite state vector) at t. Inversely, with given orbital parameters, satellite's state vector can be calculated. The number of parameters for state-based model (satellite state) and for Keplerian model (Eq. 2) of 1, 2, and N images is presented in Table 1.

Table 1. The number of parameters for state-based model and Keplerian model

	Number of parameters	
	state-based model $X_o, Y_o, Z_o, v_x, v_y, v_z, \varphi, \omega, \kappa$	Keplerian model (Eq. 2) $i, \Omega, u, r, \varphi, \omega, \kappa$
for 1 image	9	7
for 2 images	18	12
.....	.....	.....
for N images	$N(X_o, Y_o, Z_o, v_x, v_y, v_z) + N(\omega, \varphi, \kappa)$	$(i, \Omega) + N(r, u, \omega, \varphi, \kappa)$

Table 1 shows that state-based model has more parameters than Keplerian model. It means that the Keplerian model is very economical.

3. Bundle block adjustment of HRS images

The rigorous block triangulation is presented in this section, using Keplerian parameters. The advantages of rigorous model of block triangulation are the possibilities to correct sensor distortion as well as other ones caused by Earth motion and map projection, to use time-dependent equation, orbital constraints and exterior orientation registered by GPS/INS. As the disadvantages of rigorous model of block triangulation can be classified the unknown sensor physical parameters, sensor model not published by a vendor, requiring specialized software, changing mathematical model for each sensor.

Images can be acquired in the same satellite orbit by rotating sensor in the along-track direction as it happens in case of IKONOS, QuickBird, EROS, MOM 02, SPOT5, etc. (Fig. 4a, 4b), (Michalis and Dowman, 2005; Poli, 2005), by using more than one sensor looking at the Earth with different angles (Fig. 5b), (Poli, 2005) or by taking from two adjacent orbits (across-track) as in the case of SPOT1, SPOT2, SPOT4; IRS, etc. (Fig. 5a). The advantages of along-track images compared with across-track images are that they are acquired in almost the same ground and same atmospheric conditions. Along-track images are better for matching and later for conjugate point measurement. The fundamental benefit of an along-track images is to orient them simultaneously in strip triangulation.

Two models of across-track stereo images and along-track stereo images are represented in Figures 6a and 6b (Luong and Wolniewicz, 2005a).

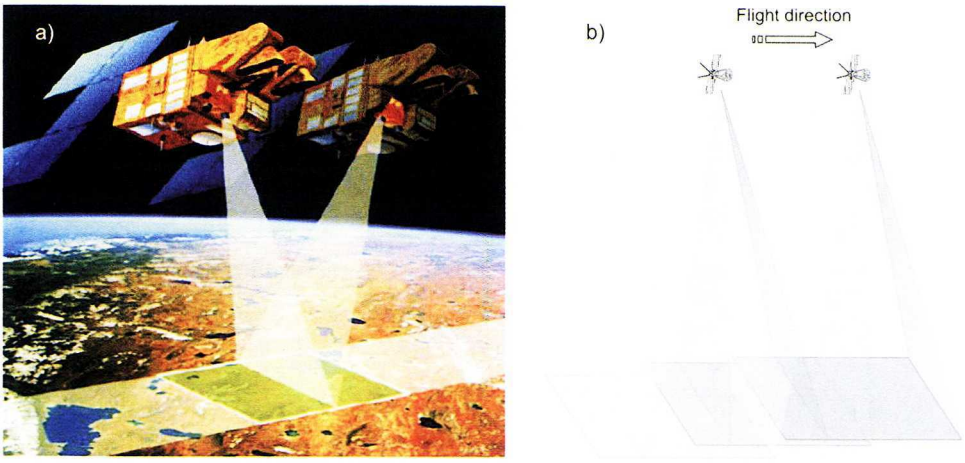

Fig. 4. Scanning in along-track orbit using three-linear array sensor (source: www.spotimage.com) a); along-track overlapping taken from one orbit using three linear array sensor b)

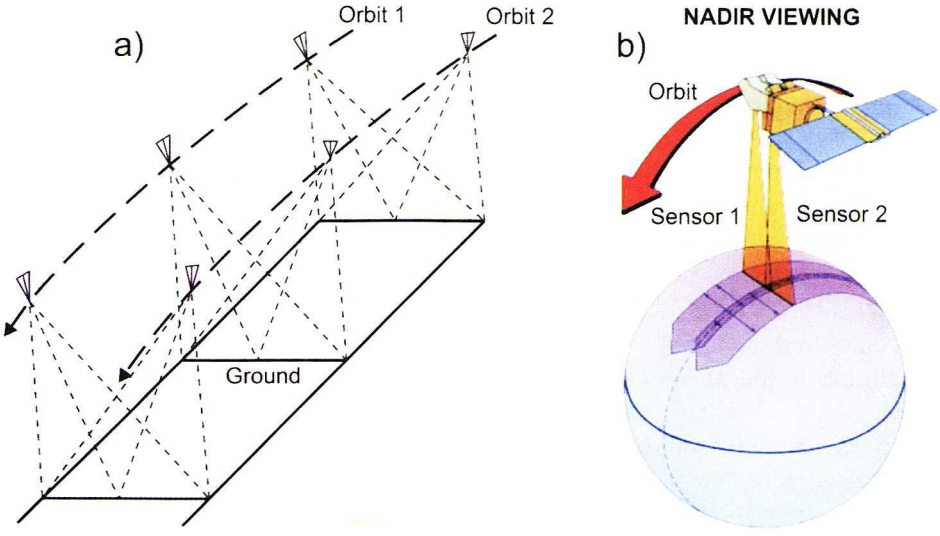

Fig. 5. Across-track overlapping taken from two orbits a); across-track overlapping taken from one orbit using two sensors b)

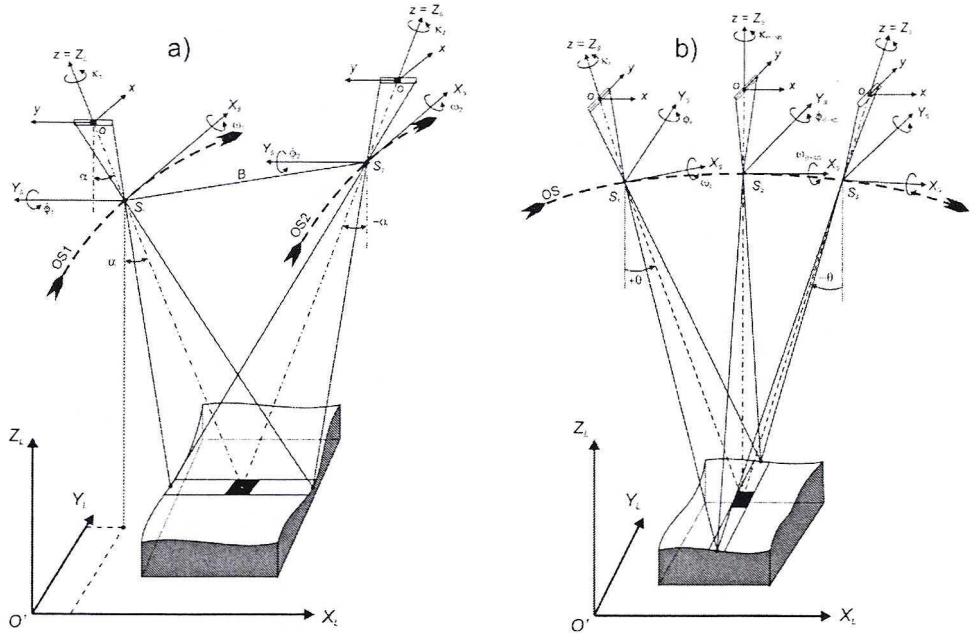

Fig. 6. Orientation elements of across-track stereomodel a);
orientation elements of along-track stereomodel b)

The satellite movement is a subject to Kepler's laws. Its orbit is of an ellipse-like shape. The radius r in (2) is a function of semi-major axis a, eccentricity e and true anomaly ϑ. For given orbit, supposed three parameters (a, e, w) remain constant (see Fig. 2). In general, for image j ($j = 1, 2, 3, \ldots, n$) of orbit (strip) k ($k = 1, 2, 3, \ldots, m$) in epoch t the equation (2) has the following form:

$$F_{xt,jk}\,[x_{jk},\ f,\ X,\ Y,\ Z,\ \theta_k,\ \varphi_{jk}(t),\ \omega_{jk}(t),\ \kappa_{jk}(t),\ i_{jk}(t),\ \Omega_{jk}(t),\ u_{jk}\ (t),\ r_{ik}(t)] = 0$$

$$F_{yt,jk}\,[y_{jk},\ f,\ X,\ Y,\ Z,\ \theta_k,\ \varphi_{jk}(t),\ \omega_{jk}(t),\ \kappa_{jk}(t),\ i_{jk}(t),\ \Omega_{jk}(t),\ u_{jk}\ (t),\ r_{ik}(t)] = 0 \tag{4}$$

Major components of dynamic motion are the Earth's rotation and the satellite movement along a defined orbit. The parameters r_{ik}, i_{jk}, Ω_{jk}, u_{jk}, φ_{jk}, ω_{jk}, κ_{jk} are time-dependent. Basing on (3) for given j image and k orbit (strip) those parameters can be modelled with second order functions of time t:

$$
\begin{aligned}
r(t) &= r_0 + r_1 t + r_2 t^2 & & r(t) = r'_0 + r'_1 l + r'_2 l^2 \\
i(t) &= i_0 + i_1 t + i_2 t^2 & & i(t) = i'_0 + i'_1 l + i'_2 l^2 \\
\Omega(t) &= \Omega_0 + \Omega_1 t + \Omega_2 t^2 & & \Omega(t) = \Omega'_0 + \Omega'_1 l + \Omega'_2 l^2 \\
u(t) &= u_0 + u_1 t + u_2 t^2 & \text{or} \quad & u(t) = u'_0 + u'_1 l + u'_2 l^2 \\
\varphi(t) &= \varphi_0 + \varphi_1 t + \varphi_2 t^2 & & \varphi(t) = \varphi'_0 + \varphi'_1 l + \varphi'_2 l^2 \\
\omega(t) &= \omega_0 + \omega_1 t + \omega_2 t^2 & & \omega(t) = \omega'_0 + \omega'_1 l + \omega'_2 l^2 \\
\kappa(t) &= \kappa_0 + \kappa_1 t + \kappa_2 t^2 & & \kappa(t) = \kappa'_0 + \kappa'_1 l + \kappa'_2 l^2
\end{aligned}
\tag{5}
$$

where l ($l = 1, 2, 3, \ldots, N$) are scan lines; r_1, r_2, i_1, i_2, Ω_1, Ω_2, u_1, u_2, φ_1, φ_2, ω_1, ω_2, κ_1, κ_2 as well as r'_1, r'_2, i'_1, i'_1, Ω'_1, Ω'_2, u'_1, u'_2, φ'_1, φ'_2, ω'_1, ω'_2, κ'_1, κ'_2 are linear coefficients; and r_0, i_0, Ω_0, u_0, φ_0, ω_0, κ_0 as well as r'_0, i'_0, Ω'_0, u'_0, φ'_0, ω'_0, κ'_0 are the parameters of base line (center line) of j image.

From (4) and (5) one can easily deduce that for an individual image the number of unknown parameters and linear coefficients equals 21, and for two along-track stereo images – 42. Suppose all the images taken from an orbit have the same view angle θ. Therefore, the total number of unknowns in an orbit (strip) having n images is $(21n+1)$. The number of unknown parameters in a block of m orbits (strips) will be $[(21n+1)]m$. There are M points in a block that need to be determined. Therefore, the total number p of unknowns to be determined in a block will be $p = [(21n + 1)]m + 3M$. If (5) is modelled with first order linear functions of t, the number of unknowns in a block will decrease by about 1/3.

After differentiating functions $F_{xt,jk}$, $F_{yt,jk}$ in (4) with respect to unknowns (parameters and ground point coordinates), basing on s image point observations in strip k, one can create the observation equation system written in the matrix form

$$\mathbf{v} = \mathbf{AX} - \mathbf{L} \quad \text{with weight matrix } \mathbf{P} \tag{6}$$

where $\mathbf{v}$ is the residual matrix ($s \times 1$) to image point coordinate observation, $\mathbf{L}$ is the observation matrix ($s \times 1$), $\mathbf{A}$ is the design matrix ($s \times p$) consisting of partial derivatives related to unknowns, $\mathbf{X}$ is the matrix ($p \times 1$) of unknowns for parametric increments and ground point coordinates, $\mathbf{P}$ is diagonal weight matrix ($s \times s$), p is the number of unknowns.

The matrix equation (6) is written for the following groups of points: ground control points (GCP) and independent check points (ICP), conjugate points in the block and other interesting points, namely the new ground points (NGP).

The estimated matrix of unknowns $\hat{\mathbf{X}}$ is obtained as a solution of the normal equation system calculated from (6).

$$\hat{\mathbf{X}} = (\mathbf{A}^{\mathrm{T}}\mathbf{PA})^{-1}\mathbf{A}^{\mathrm{T}}\mathbf{PL} \tag{7}$$

From (1a) and (5) one can draw a number of conclusions:

- there is a strong correlation between the linear unknowns X_S, Y_S, Z_S and angular unknowns ω, φ, κ. For example, a small change in φ will cause a big change in X_S. The strong correlation induces singularity of the coefficient matrix of normal equations, ill-conditioning of the normal equation and practical zeroing of some eigenvalues in the eigenvalue matrix. Accordingly, the RMSE value of least-squares estimated value $\hat{\mathbf{X}}$ become very large and least-squares estimator is no more an optimum one; the main reason that caused strong correlation among image orientation parameters is narrow field of view (FOV) of image. For example, FOV for IKONOS, QuickBird and SPOT image equal to 0.93°, 2.12° and 4.13°, respectively;
- two groups of angular unknowns ω, φ, κ and Ω, i, u simultaneously occurring in (1a) are also strongly correlated what causes the ill-conditioning of normal equations;
- there is also an internal correlation between unknown angular parameters which became modelled by second order functions of time t (5). It reduces the accuracy of estimated value $\hat{\mathbf{X}}$.

In order to overcome the weak geometry caused by narrow FOV and strong correlations between the unknown parameters to be determined finding the suitable method of adjustment for building bundle block of HRS, and/or finding the additional constraints to keep satellite in its plane orbit is needed.

The solution for exact building of bundle block of HRS are described in the following section.

3.1. Ridge-stein estimator for bundle block adjustment of HRS images

For reducing the influences of parameter correlations on accuracy of estimated value $\hat{\mathbf{X}}$ one can use the combined ridge-stein estimator. Experimental results performed by Wang et al. (2004) show that the combined ridge-stein estimator can effectively overcome the strong correlation among exterior orientation elements and reach high reliability, stability and accuracy. Three formulae for ridge, stein and combined ridge-stein estimation values $\hat{\mathbf{X}}_R(k)$, $\hat{\mathbf{X}}_S(c)$, $\hat{\mathbf{X}}_{CRS}(d)$ are as follows:

$$\hat{\mathbf{X}}_R(k) = (\mathbf{A}^T\mathbf{P}\mathbf{A} + \mathbf{K}\mathbf{I})^{-1}\mathbf{A}^T\mathbf{P}\mathbf{L} \tag{8}$$

$$\hat{\mathbf{X}}_S(c) = c(\mathbf{A}^T\mathbf{P}\mathbf{A})^{-1}\mathbf{A}^T\mathbf{P}\mathbf{L} \tag{9}$$

$$\begin{aligned}\hat{\mathbf{X}}_{CRS}(d) &= (\mathbf{A}^T\mathbf{P}\mathbf{A} + \mathbf{I})^{-1}(\mathbf{A}^T\mathbf{P}\mathbf{L} + d\mathbf{I})\hat{\mathbf{X}} \\ &= \mathbf{Q}(\mathbf{\Pi} + \mathbf{I})^{-1}(\mathbf{\Pi} + d\mathbf{I})\mathbf{Q}^T\hat{\mathbf{X}}\end{aligned} \tag{10}$$

where **I** is the unit matrix, **K** is the ridge parameter vector (elements $k_i > 0$), c is the stein parameter ($c > 0$), d is the combined ridge-stein parameter ($0 < d < 1$), and **Q** and **Π** are the eigenvector and eigenvalue matrices, respectively.

Experimental results (Wang et al., 2004) confirmed that strong correlation among exterior orientation elements of HRS images taken from linear pushbroom sensor causes the normal equation ill-conditioned and least squares estimation values no longer optimal. The use of the new biased estimator that is the combined ridge-stein estimator can effectively reduce the ill-conditioning problem and improve orientation precision.

3.2. Orbital constraints

Because of the narrow field of view (FOV) of sensor causing a weak geometry and strong correlations between the unknown parameters the adjustment process does not converge. To overcome that problem the addition of orbital constraints is needed to keep the orbital position of the sensor within statistical limits of the expected nominal orbit (Fritsch and Stallmann, 2004).

The image of point S (satellite) on the Earth is a point O' (Fig. 2) that determines the ground scene centre (GSC) with co-ordinates Λ, Φ, ϑ. Three orbital constraints derived from known orbit relation can be used as follows:

1. The geocentric distance constraint keeps the satellite in orbit:

$$r^2(X_S, Y_S, Z_S) - r^2(\vartheta_S) = 0 \qquad \text{with the weight } p_r \tag{11}$$

2. The true anomaly ϑ restricts the movement of the reference position along the orbit:

$$\vartheta(X_S, Y_S, Z_S) - \vartheta_S = 0 \qquad \text{with the weight } p_\vartheta \tag{12}$$

3. The Λ – geocentric longitude restricts the rotation of the orbit plane:

$$\Lambda(X_S, Y_S, Z_S) - \Lambda_S = 0 \qquad \text{with the weight } p_\Lambda \tag{13}$$

where ϑ_S, Λ_S and $r^2(\vartheta_S)$ are the reference values of nominal orbit and nominal geocentric distance, respectively, considered as pseudo-observations; $r^2(X_S, Y_S, Z_S)$, $\vartheta(X_S, Y_S, Z_S)$ and $\Lambda(X_S, Y_S, Z_S)$ are the geocentric distance, true anomaly and geocentric longitude, respectively, derived from unknown reference position. Three equations (11), (12) and (13) are transformed to the form of (6) and further added to the observation equations. The next step of block adjustment becomes realized according to (8), (9) or (10).

In the Institute of Photogrammetry and Cartography of the Warsaw University of Technology a bundle block adjustment of HRS images described by Keplerian parameters has been carried out. In the near future first results of will be presented.

4. Conclusions

Bundle block adjustment of very high resolution satellite images based on orbit mechanism has recently became one of the important research directions. Block of HRS images built with rigorous (parametric or physical) model has more advantages related with possibilities to reduce different systematic errors. In the result, the accuracy of ground point co-ordinates determined from block of HRS images will be increased. One of the important tasks of block adjustment based on Keplerian parameters is to overcome strong correlation among exterior orientation elements. For that purpose the use of the ridge-stein estimator has been proposed. To further improve an accuracy of determined ground point co-ordinates in block, the correction of image coordinates caused by Earth's motion, providing orbital constraints related with a satellite position in space and optimum of ground control point (GCP) configuration have been continuously studied.

The Keplerian model has also a special meaning for in-flight calibrating of measurement systems such as scanner, GPS and INS (inertial navigation system) assembled on the satellite. After long time working and due to different reasons in satellite's orbit those systems become disturbed. Corrections to their measurement parameters will be necessary.

The difficult problem with using the Keplerian model is the need to have the raw image with ephemeris data. Some high resolution satellite image vendors do not intend, however, to release those data. They provide users with geo-rectified images (for example IKONOS) with minimum information about the satellite's movement in its orbit. It means the lack of geometry at the time of imaging which makes it very difficult to use the Keplerian model for geometric correction of those images. Other rigorous methods for solving this problem are under investigation.

Acknowledgements

The author would like to thank Prof. S. Białousz from the Institute of Photogrammetry and Cartography, Warsaw University of Technology for helpful consultation and suggestions.

References

Dial D., Grodecki J., (2003): *Block adjustment of high-resolution satellite images described rational function*, Photogrammetric Engineering and Remote Sensing, Vol. 69, No 1, pp. 59-68.

Dial D., Grodecki J., (2004): *Satellite image block adjustment simulations with physical and RPC camera models*, ASPRS Annual Conference Proceedings, May 2004, Denver, Colorado (CD).

Dial D., Grodecki J., (2005): *RPC replacement camera models*, International Archives of the Photogrammetry, Remote Sensing and Spatial Information Sciences, Vol. 34, part XXX.

Dowman I., Michalis P., (2003): *Generic rigorous model for along track stereo satellite sensors*, ISPRS Workshop Proceedings, May 2003, Hannover (CD).

Fritsch D., Stallmann D., (2004): *Rigorous photogrammetric processing of high resolution satellite imagery*, IAPRS of 20th Congress, Commission I, WG V/5, Istanbul, Turkey (CD).

Grodecki J., Dial D., Lutes J., (2003): *Error propagation in block adjustment of high-resolution satellite images*, ASPRS Annual Conference Proceedings, May 2003, Anchorage, Alaska (CD).

Grodecki J., Dial D., Lutes J., (2004): *Mathematical model for 3D feature extraction from multiple satellite images described by RPCs*, ASPRS Annual Conference Proceedings, May 2004, Denver, Colorado (CD).

James L., (2004): *Satellite image block adjustment simulations with physical and RPC camera models*, IAPRS of 20th Congress, Commission I, WG V/5, Istanbul, Turkey (CD).

Jacobsen K., (2005): *High resolution satellite imaging systems - overview*, Proceedings of ISPRS workshops, Hannover, Germany (CD).

Kaczyński R., Ewiak I., (2005): *Correction IKONOS and QuickBird data for orthomaps generation*, 26th Asia Conference of Remote Sensing, Ha Noi, Vietnam (CD).

Luong C.K., Wolniewicz W., (2005a): *Very high resolution satellite image triangulation*, 26th Asia Conference of Remote Sensing, Ha Noi, Vietnam (CD).

Luong C.K., Wolniewicz W., (2005b): *Geometric models for satellite sensors*, Geodesy and Cartography, Warsaw, Vol. 54, No 4, pp. 191-203.

Madami M., (2005): *Satellite image triangulation*, ISPRS workshop proceeding of Commission I, WG I/5, May 2005, Hannover (CD).

Michalis P., Dowman I., (2004): *A rigorous model and DEM generation for SPOT5-HRS*, IAPRS of 20th Congress, Commission I, WG V/5, Istanbul, Turkey (CD).

Michalis P., Dowman I., (2005): *A model for along track stereo sensors using rigorous orbit mechanics*, ISPRS workshop proceedings of Commission I, WG I/5, May 2005, Hannover (CD).

Passini P.M., Jacobsen K., (2006): *Accuracy investigation on large blocks of high resolution images*, IAPRS, Band XXXVI/5, WG I/5, Paris.

Passini P.M., Blades A., Jacobsen K., (2005): *Handing of large blocks of high resolution space images*, ISPRS workshop proceedings of Commission I, WG I/5, May 2005, Hannover (CD).

Poli D., (2005): *Modelling of spaceborne linear array sensor*, PhD Thesis in the Institute of Geodesy and Photogrammetry, Zurich, Switzerland, 184 p.

Wang T., Zhang Y-S., Zhang Y., (2004): *Combined ridge-stein estimator in exterior orientation for linear pushbroom imagery*, IAPRS of 20th Congress, Commission IV, WG IV/7, Istanbul, Turkey (CD).

Wolniewicz W., Luong C.K., (2006): *Geometric modelling of VHRS imagery*, ISPRS International Calibration and Orientation Workshop EuroCOW 2006, 25–27 January 2006, WG I/3, Castelldefels, Spain (www.isprs.org/commission 1/uroCOW6).

Yamakawa T., Fraser C.S., (2004): *The affine projection model for sensor orientation: experiences with high-resolution satellite imagery*, IAPRS of 20th Congress, Commission I, WG V/5, Istanbul, Turkey (CD).

Zhang J., Zhang Y., Cheng Y., (2004): *Block adjustment based on new strict geometric model of satellite images with high resolution*, IAPRS of 20th Congress, Commission I, WG V/5, Istanbul, Turkey (CD).

Matematyczny model bloku wysokorozdzielczych obrazów satelitarnych z wykorzystaniem orbitalnych warunków keplerowskich

Luong Chinh Ke

Politechnika Warszawska
Instytut Fotogrametrii i Kartografii
Plac Politechniki 1, 00-661 Warszawa
e-mail: lchinhke@gazeta.pl

Streszczenie

Od początku 21 wieku wysokorozdzielcze obrazy satelitarne z satelitów takich jak IKONOS, QuickBird (USA), ALOS (Japonia), EROS (Izrael), SPOT5 (Francja), IRS (India) itd. są stosowane komercyjnie dla różnych celów gospodarczych. Obrazy satelitarne Pléiades (Francja) z pikselem terenowym poniżej metra (GSD = 0.71 m), ClearView (GSD = 0.47 m) i GeoEye (GSD = 0.41 m), jakie pojawią się w najbliższym czasie na rynku światowym, stworzą nowe możliwości wykorzystania super wysokorozdzielczych obrazów satelitarnych SHRS (Super High Resolution Satellite) do opracowania map wielkoskalowych, np. 1:5 000.

W trakcie opracowania wysokorozdzielczych obrazów potrzebne są pewne liczby fotopunktów wyznaczanych np. metodą DGPS. W niniejszej pracy zaproponowano metodę bloku triangulacji z obrazów HRS, której użycie prowadzi do zmniejszenia kosztów pomiaru fotopunktów. Aby zbudować blok triangulacji z obrazów HRS należy rozpoznać i zbadać modele opisujące zależność pomiędzy obrazem i terenem. W pracy przedstawiono opis modelu Keplera obrazu, który obecnie jest przedmiotem badań w różnych ośrodkach naukowych na świecie. W dalszej części przedstawiono algorytm budowy bloku triangulacji z obrazów HRS metodą parametryczną z uwzględnieniem elementów kątowych orbity satelity poruszającego zgodnie z prawami Keplera. Dla zmniejszenia wpływu korelacji pomiędzy zewnętrznymi elementami orientacyjnymi obrazu, zaproponowano użycie estymatora ridge-stein. Z powodu silnej korelacji pomiędzy elementami orientacji obrazu oraz geometrii wąskiego kąta widzenia obiektywu sensora proces wyrównania może nie być zbieżny. Aby pokonać ten problem, do układu poprawek zostały wprowadzone warunkowe równania orbitalne, które mają za zadanie utrzymanie satelity na orbicie.

Praca nad budową bloku wysokorozdzielczych obrazów satelitarnych jest w toku realizacji w Instytucie Fotogrametrii i Kartografii Politechniki Warszawskiej. Pierwsze wyniki zostaną przedstawione w najbliższym czasie.